Joule Heating a Palladium Nanowire Sensor for Accelerated Response and Recovery to Hydrogen Gas

*Fan Yang, David K. Taggart, and Reginald M. Penner**

The properties of a single heated palladium (Pd) nanowire for the detection of hydrogen gas (H_2) are explored. In these experiments, a Pd nanowire, 48–98 μm in length, performs three functions in parallel: 1) Joule self-heating is used to elevate the nanowire temperature by up to 128 K, 2) the 4-contact wire resistance in the absence of H_2 is used to measure its temperature, and 3) the nanowire resistance in the presence of H_2 is correlated with its concentration, allowing it to function as a H_2 sensor. Compared with the room-temperature response of a Pd nanowire, the response of the heated nanowire to hydrogen is altered in two ways: First, the resistance change ($\Delta R/R_0$) induced by H_2 exposure at any concentration is reduced by a factor of up to 30 and second, the rate of the resistance change – observed at the beginning (''response'') and at the end (''recovery'') of a pulse of H_2 – is increased by more than a factor of 50 at some H_2 concentrations. Heating nearly eliminates the retardation of response and recovery seen from 1–2% H_2, caused by the $\alpha \rightarrow \beta$ phase transition of PdH_x, a pronounced effect for nanowires at room temperature. The activation energies associated with sensor response and recovery are measured and interpreted.

Keywords:
- hydrogen sensors
- Joule heating
- nanocrystalline materials
- palladium nanowires

1. Introduction

Hydrogen safety sensors are tasked with the detection of leaked H_2 gas in the many industrial environments in which H_2 is in use. Since the lower explosion limit for H_2 in air is 4%,[1] these sensors must detect H_2 within seconds at lower concentrations. The Department of Energy performance targets for H_2 safety sensors, disclosed in a 2009 request for proposals (RFP),[2] specify a response time of 1 s at 4% H_2 and 60 s at 1%, and a recovery time of 60 s independent of concentration. This RFP also specifies the H_2 range over which the sensor must function as 0.4% to 4% H_2. [2] It further asserts[2] that no existing H_2-sensing technology has achieved this combination of performance metrics while simultaneously meeting the requirement for a cost of <$40/sensing node.

Palladium (Pd) and Pd alloy resistors are excellent candidates for safety sensors because the simplicity of these devices can render them both inexpensive and rugged. H_2 sensors consisting of Pd-based alloy thin-film resistors were first described by Hughes and Schubert[3] in 1992. In that study, resistors with thicknesses in the 50-nm range produced response times of ≈10 s at 4% H_2 and ≈20 s at 1% H_2 while achieving a limit of detection below 0.1%.[3] In an attempt to accelerate the response and recovery of resistor-based H_2 sensors, we[4–8] and others[9–11] have studied the properties of Pd nanowires for detecting H_2. A recurrent problem[4–8] with this approach has been the spontaneous fracture of these nanowires upon exposure to H_2.

We have recently described[8] the preparation of nanocrystalline Pd (nc-Pd) nanowires that resist fracture upon exposure to hydrogen gas at any concentration. Such nc-Pd nanowires exhibit a resistance increase of ≈15–20% at 10% H_2 and can detect H_2 in the low ppm range at room temperature. [8] The smallest of these nc-Pd nanowires have response times of 6 s at

[*] Prof. R. M. Penner, F. Yang, D. K. Taggart
Department of Chemistry, University of California
Irvine, CA 92697 (USA)
E-mail: rmpenner@uci.edu

DOI: 10.1002/smll.201000145

small NANO MICRO

4% and 20 s at 1% H_2. Similar performance for single Pd nanowires has recently been reported by Offermans et al.,[10] who were also the first to explore the effect of Joule self-heating to accelerate the H_2 sensing response of the nanowire. They showed that the response time could be reduced from the room-temperature value by applying a larger measurement voltage to the nanowire of up to 800 mV. For example, Offermans et al. showed that the response time to 2.4% H_2 decreased from 12 s to 4 s as the measurement voltage was increased from 50 mV to 800 mV, producing an estimated increase in the nanowire temperature of 100 K.[10]

In this Full Paper, we demonstrate that Joule heating at higher applied voltages up to 19 V can be used to obtain even more dramatic reductions in the response and recovery time for Pd nanowires of up to a factor of 50. We also quantify the loss of measurement sensitivity that accompanies Joule heating and measure the activation energies associated with response and recovery of a Pd nanowire hydrogen sensor.

2. Results and Discussion

Ultralong ($l > 48$ μm) nc-Pd nanowires were patterned on glass substrates using the lithographically patterned nanowire electrodeposition (LPNE) method.[12–14] An ethylenediaminetetraacetic acid (EDTA)-containing Pd plating solution was used for the electrodeposition of the nc-Pd nanowire because, as we have recently demonstrated,[8] nc-Pd nanowires electrodeposited from an EDTA-containing electrolyte are impervious to fracture during exposure to H_2. A source meter (Keithley 2400) and a multimeter (Keithley 2000) were used in parallel to apply a voltage associated with current flow (E_{app}) and to measure this voltage, respectively, in order to eliminate the contact resistance from the voltage measurement (Figure 1a). Sensors were fabricated by isolating a 49-to-98-μm length of a single nc-Pd nanowire on glass using two evaporated gold stripes (Figure 1b). Scanning electron microscopy (SEM) and atomic force microscopy (AFM) were used to determine the width and height of these nanowires, respectively (Figure 1d–f). The mean width and height for the three nanowires were 75 ± 5 nm $\times$ 27 ± 4 nm, 54 ± 5 nm $\times$ 52 ± 2 nm, and 183 ± 9 nm $\times$ 94 ± 2 nm. Other properties of these nanowires, including their electrical resistances and electrically isolated lengths, are summarized in Table 1.

At the beginning of this study we wished to know the temperature distribution along the axis of a glass-supported Pd nanowire produced by Joule heating. To answer this question we calculated the temperature distribution of the nanowires and the glass support using three-dimensional (3D) finite-element analysis (COMSOL Multiphysics 3.5a). For example, the temperature distribution in the vicinity of the largest nanowire we investigated (94 × 183 nm) is shown in Figure 2a for an applied voltage biase, $E_{app} = 5.6$ V, corresponding to 4.1 mW of dissipated power. This calculation explicitly considers that the Pd nanowire is supported on glass and surrounded by air. It also assumes that both ends of the nanowire are maintained at 300 K by the electrical contacts. The resulting temperature-versus-distance plots (Figure 2b) reveal that within 10 μm of the electrical contacts, the wire temperature reaches a value that is invariant along the wire axis. In the case of the 94 × 183-nm nanowire, this temperature was elevated above ambient (assumed to be 300 K) by ≈0.35 K for $E_{app} = 0.36$ V and 83.8 K for $E_{app} = 5.6$ V, for example. This characteristic temperature is proportional to the dissipated power, i^2R, and therefore proportional to $(E_{app})^2$ (Figure 2e, simulation).

The actual mean temperature of the nanowire can be accurately measured using the resistance of the nanowire itself. We calibrated the 94 × 183-nm Pd nanowire by placing it in an oven and measuring the wire resistance as the oven temperature was varied from 293 K to 550 K in the absence of H_2 (Figure 2c). From these data, a temperature coefficient of resistance, $\alpha = 1.35 \pm 0.01 \times 10^{-3}$ K^{-1}, was obtained (Fig. 2d). This value is much larger than that measured by Offermans et al.[10] ($\alpha = 5.6 \pm 0.2 \times 10^{-4}$ K^{-1}), but just 42% of the value for bulk Pd (3.2×10^{-3} K^{-1}).[15] A comparison of the wire temperature measured from the wire resistance (Figure 2e, experiment) and the maximum temperature predicted by the simulation (Figure 2e, simulation) shows excellent agreement. Simulations for

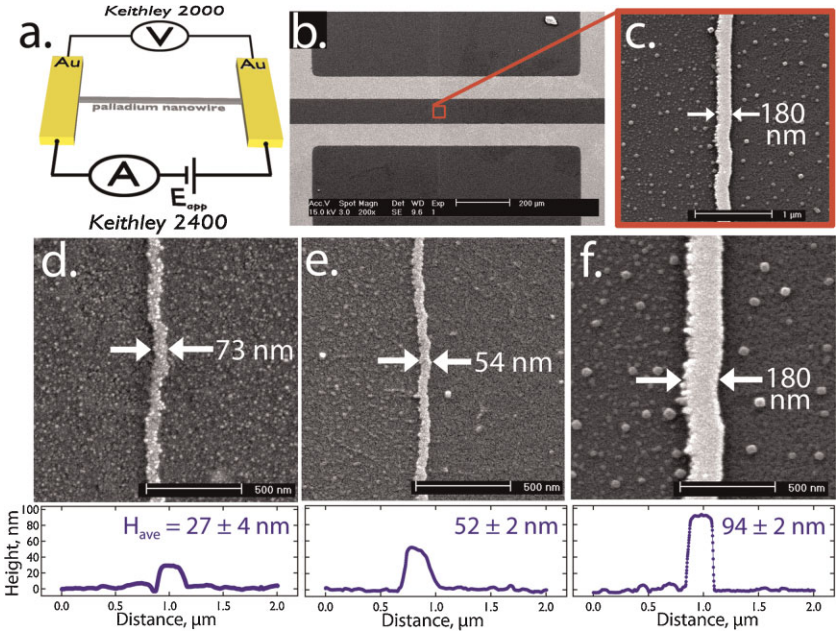

Figure 1. The single Pd nanowire H_2 sensor employed in these studies: a) Schematic diagram of the 4-point probe measurement configuration used for nanowire resistance measurements involving ohmic wire heating. b) SEM image of the sensor showing electrical contacts and the single nanowire. A 48–100-μm length of this nanowire was isolated using evaporated gold contacts. d–f) Higher-magnification SEM images showing the three Pd nanowires investigated in this study. Shown below each image is a line scan acquired using an atomic force microscope showing the wire height. The mean height (H_{ave}) with the standard deviation is indicated for ten measurements.

Table 1. Dimensions and electrical resistances of the three nanowires investigated at T_{hot}.

Nanowire lateral dimensions $W \times H$ [nm]	Length[a] [μm]	R[b] [kΩ]	E_{app} [V]	P[c] [mW]	T_{hot}[d] [K]
$183 \pm 9 \times 94 \pm 2$	91	7.6	5.6	4.1	384
$54 \pm 5 \times 52 \pm 2$	48	80	18	4.0	410
$75 \pm 5 \times 27 \pm 4$	98	88	19	4.0	428

[a] Electrically isolated nanowire length. [b] Resistance measured at T_{hot}. [c] Power dissipated at T_{hot}. [d] Temperature of the nanowire at E_{app} estimated using a FEMLab simulation. In the case of the 94×183-nm nanowire, the temperature estimate is confirmed using the measured value of α.

the other two nanowires employed in this study, with smaller cross sections of 27×75 nm and 52×54 nm, produce mean wire temperatures of 428 K and 410 K, respectively, using $E_{app} = 19$ V and 18 V. The power dissipated by all three of these nanowires was ≈ 4 mW.

Joule heating alters the response of the 94×183-nm nanowire to H_2 in two principal ways (Figure 3a): 1) Response to, and recovery from, hydrogen exposure are both accelerated, and 2) the sensitivity of the wire resistance to hydrogen exposure is reduced. These trends are preserved for two different hydrogen concentrations – one above (5.0% H_2) and one below (0.5% H_2) the α-to-β phase transition for Pd hydride that occurs at 1–2% H_2. When the temperature dependence of the response time is plotted (Fig. 3b), we arrive at an important conclusion: The marginal reduction in response time, τ, with increasing temperature becomes smaller with increasing temperature, T. For example, an increase in T to 324 K from 300 K causes τ for 5% H_2 to be reduced from 114 s to 31 s ($\tau_{324}/\tau_{300} = 0.27$) but increasing the temperature to 340 K produces a further reduction in τ of just 13 s (to 18 s, or $\tau_{340}/\tau_{300} = 0.16$). The curvature of the τ versus T plots means that the initial temperature increase of 20 K has a stronger influence on the response time than subsequent increments of 20 K. Qualitatively the same effect is seen for recovery (Figure 3c).

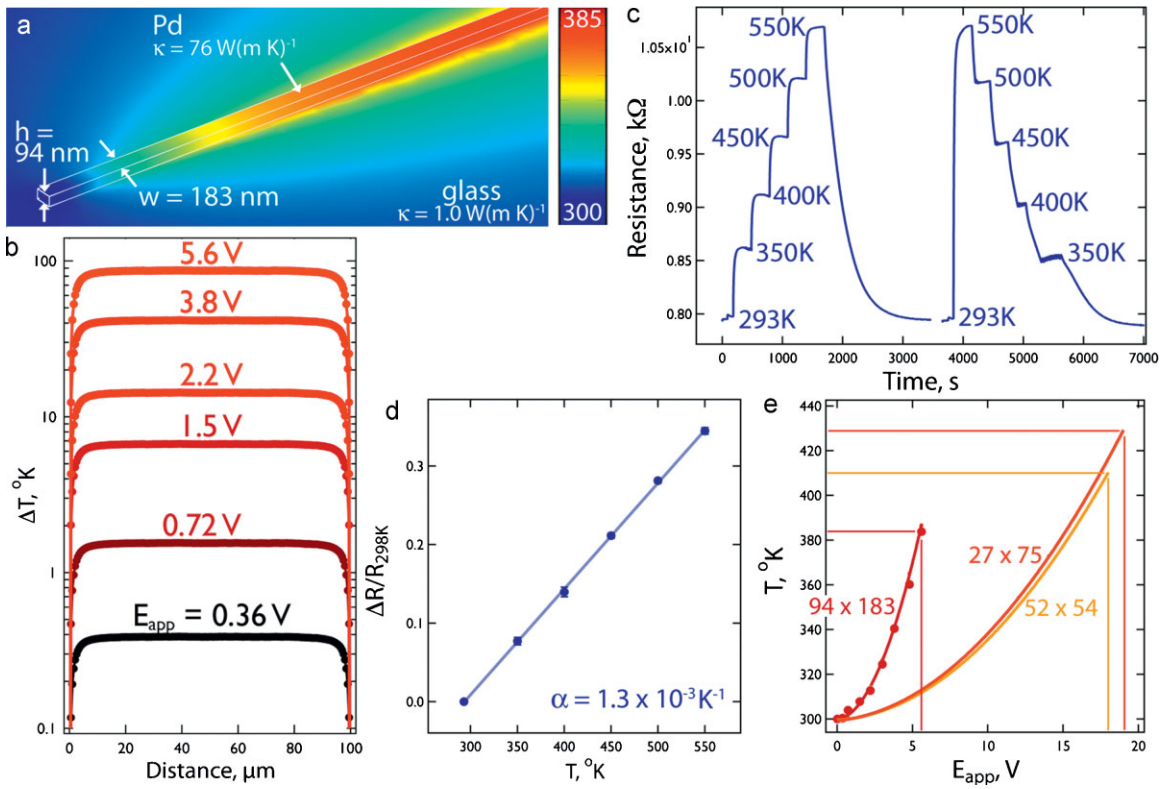

Figure 2. The Joule heating, and measurement of temperature, for a Pd nanowire on glass. a) 3D model in COMSOL of a Pd nanowire (lateral dimensions: 94×183 nm) on a planar glass surface showing the temperature distribution on the wire during current flow ($E_{app} = 5.6$ V, $I \approx 700$ μA). The color indicates the surface temperature based on the color coded key shown to the right. b) Plots of ΔT versus distance along the axis of the nanowire shown in (a) measured for a range of applied voltages (E_{app}), as indicated. c) Resistance calibration of a Pd nanowire (lateral dimensions: 94×183 nm) for the measurement of temperature in an oven. d) Change in wire resistance normalized by the initial resistance ($\Delta R/R_o$) plotted versus temperature for the wire and data shown in (c). The temperature coefficient of resistance, α, is indicated. e) COMSOL simulations of the maximum wire temperature versus E_{app} for the three nanowires (with indicated dimensions) probed in this study. The wire temperature corresponding to T_{hot} in each case (Table 1) is indicated. Also shown is the experimentally measured result for the 94×183-nm wire (data points). The indicated voltage in each case corresponds to a power dissipation of 4 mW.

small NANO MICRO

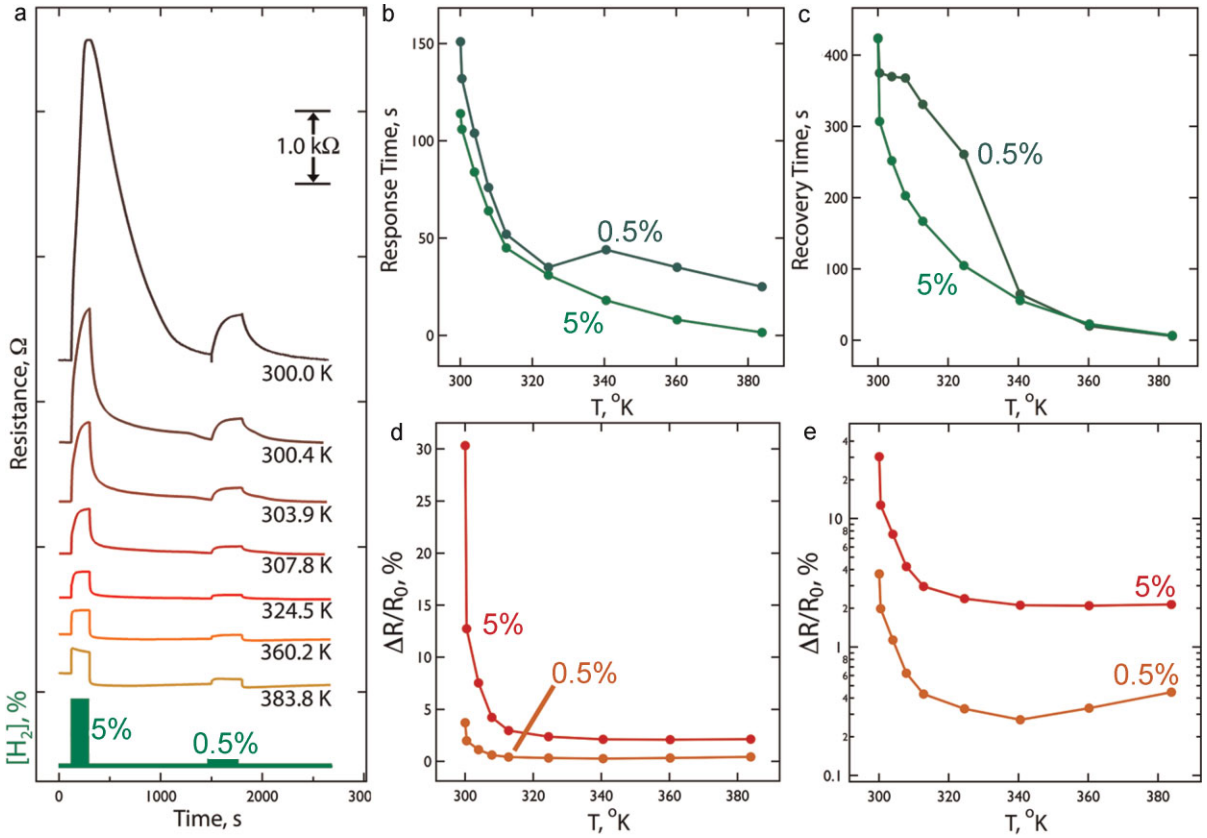

Figure 3. Influence of Joule heating on the response to hydrogen gas of a Pd nanowire (94 × 183 nm). a) Resistance versus time for the detection of hydrogen at two concentrations – 0.5% (below the α → β phase transition) and 5% (above it). The sensor traces are displaced along the resistance axis to improve clarity. b) Response time versus temperature at 5% and 0.5% H_2, derived from the raw data shown in (a). c) Recovery time versus temperature. d) Resistance change ratio, $\Delta R/R_0$, versus temperature. e) $\Delta R/R_0$ versus T plotted using log-linear axes.

The magnitude of the resistance change induced by H_2 exposure, $\Delta R/R_0$, is also reduced dramatically in the temperature range just above ambient (Figure 3d,e). The shape of this curve is similar to the composition versus temperature plots first reported by Sieverts and Danz in 1937.[16] Since the resistance of PdH_x is approximately linearly related to x [17] the rapid decrease in sensitivity seen above 300 K most likely coincides with the α/β coexistence region, qualitatively as expected from the phase diagram.[17] That is, the pressure plateau for the α-to-β phase transition is 1–2% at room temperature, so 5% H_2 induces the phase transition and causes a large resistance change. Increasing the temperature slightly, to say 320 K, moves the pressure plateau for the phase transition above 5% so that exposure of the nanowire to this concentration causes a much smaller composition and resistance change, as seen in Figure 3d,e. The sharp drop in resistance seen in Figure 3d,e is prima facie evidence that the α-to-β phase transition occurs in these nanocrystalline nanowires in spite of the fact that it has been reported previously[18] to be suppressed in nanocrystalline Pd films.

A comparison of a hot (384 K) and a room-temperature Pd nanowire over a broader range of H_2 concentrations (Figure 4) reveals two additional nuances. First, at 300 K, these Pd nanowires are unable to discriminate different H_2 concentrations above 4% (Figure 4a). We have previously reported this "saturation" of the wire response at high H_2 concentrations,[8] but this effect was not seen for the Pd nanowires evaluated by Offermans et al.[10] The hot nanowire (Figure 4b) produces $\Delta R/R_0$ in direct proportion to the $[H_2]$ over this entire concentration range, but appreciable "drift" of the baseline resistance to lower-resistance values also occurs in all three nanowires at these high H_2 concentrations but the reason for this shifting baseline is unknown at present. Second, the reduced limit-of-detection for H_2 (LOD_{H2}) at the 300 K nanowire is in the range of 2–5 ppm but the 384 K nanowire shows a LOD_{H2} of 400–500 ppm – a direct consequence of the reduced solubility of H_2 in Pd at elevated temperature.[16]

The influence of Joule heating on the sensitivity, response, and recovery times is summarized for all three nanowires in Figure 5. The sensitivity loss at T_{hot}, calculated as $(\Delta R/R_0(RT))/(\Delta R/R_0(T_{hot}))$ is quasi-independent of $[H_2]$ and in the range of 8 to 38 (Figure 5a). This latter value is seen for the smallest nanowire at its LOD of 200 ppm. The sensitivity of the two smallest nanowires is significantly lower than for the largest nanowire as a consequence, we believe, of their higher T_{hot} values of 410 K (54 × 52 nm) and 428 K (27 × 75 nm) versus 384 K (94 × 183 nm, Table 1), but a lower LOD of 200 ppm is achieved for each. The acceleration of response (Figure 5b) and recovery (Figure 5c) is most pronounced for the two smaller nanowires, and the largest accelerations are seen at the $[H_2] = 1\%$ threshold for the α → β phase transition. For example, the response times for the 27 × 75-nm nanowire were accelerated by a factor of 11 at $[H_2] = 10\%$, by a factor of 52 at $[H_2] = 2\%$, and by 23 at 200 ppm. In fact, the retardation of the

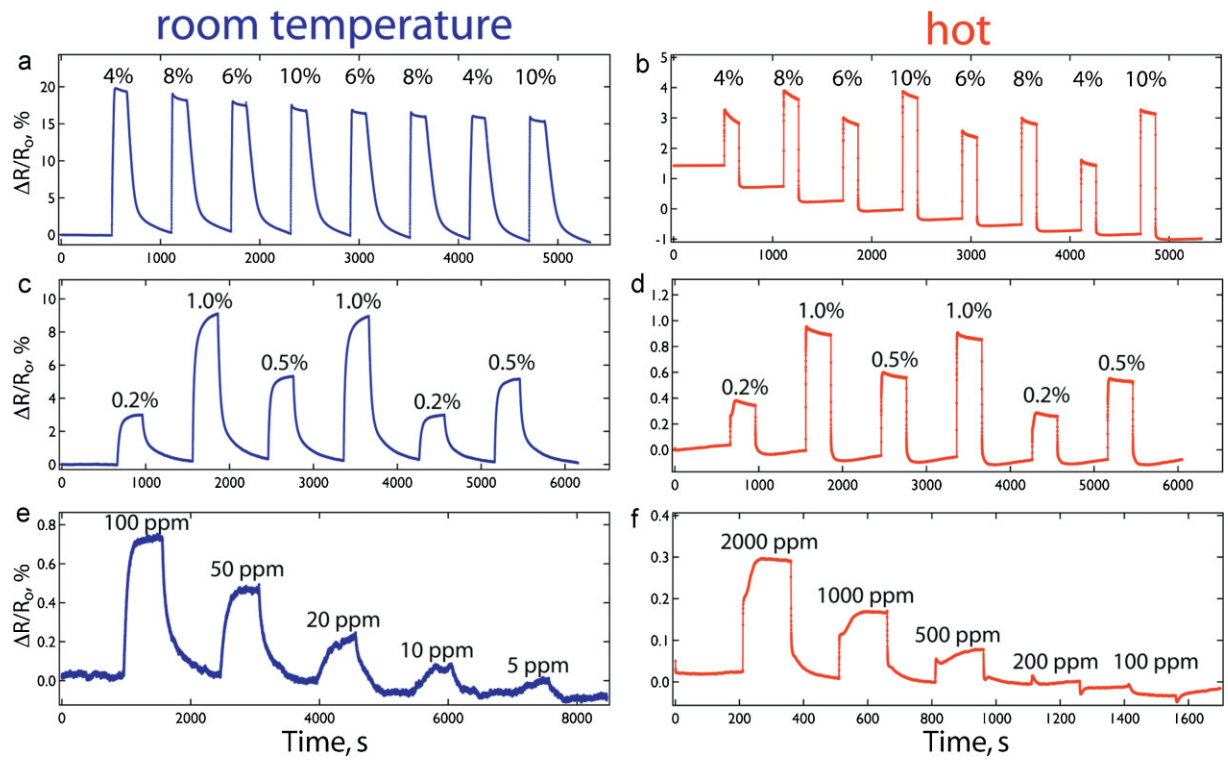

Figure 4. Raw sensing response, $\Delta R/R_0$, versus time for a single 94 × 183-nm Pd nanowire at room temperature (≈294 K) and at 384 K ("hot"). The $[H_2]$, (v/v%) for each exposure is indicated.

nanowire response observed at room temperature for $1\% < [H_2] < 3\%$ is nearly eliminated at T_{hot} for all three nanowires (Figure 5b). For reasons discussed in the next paragraph, generally speaking, recovery times are more strongly affected by heating than response times for the same nanowire. For example, the recovery times of the 27 × 75-nm nanowire were accelerated by a factor of 40 at $[H_2] = 10\%$, by a factor of 38 at $[H_2] = 2\%$, and by 54 at 200 ppm. However, response time is a more important metric than recovery time for the performance of H_2 safety sensors for obvious reasons. The DOE guideline for recovery is 60 s independent of concentration.[2] The smallest two nanowires characterized here meet this standard for their entire response ranges spanning more than four orders of magnitude in $[H_2]$ (Figure 5c).

What chemical processes limit the rate at which a single Pd nanowire responds to, and recovers from, exposure to hydrogen? The temperature dependence of these processes provides some insight into the origin of these kinetic bottlenecks. Joule heating accelerates both response to, and recovery from, hydrogen because these processes are thermally activated. If we approximate the rates associated with the response and recovery processes (Figure 3b,c) as $1/\tau$, where τ is the response time, we find that Arrhenius plots of $\mathrm{Ln}(1/\tau)$ versus $1/T$ are approximately linear for both response and recovery at

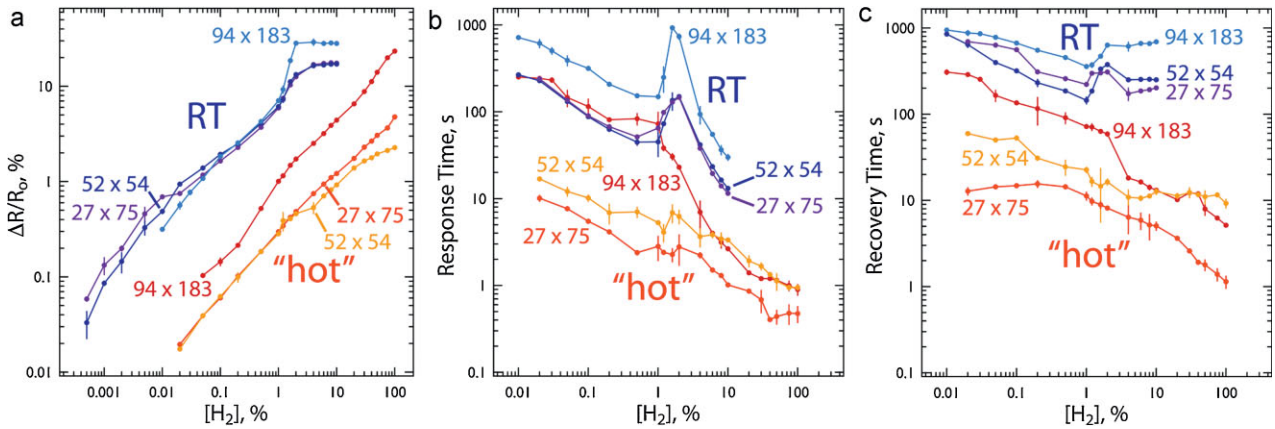

Figure 5. Summary of hydrogen sensing data for three nanowires at room temperature (RT ≈ 294 K) and at T_{hot} (Table 1). a) $\Delta R/R_0$ versus $[H_2]$, (v/v%). b) Response time versus $[H_2]$, (v/v%). c) Recovery time versus $[H_2]$, (v/v%).

small NANO MICRO

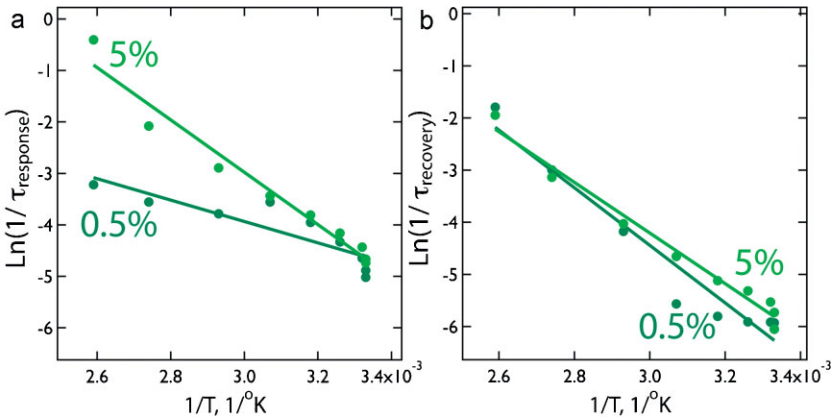

Figure 6. Arrhenius plots for the response rate (a) and the recovery rate (b) of the 94 × 183 nm Pd nanowire. Activation energies derived from the slopes of these plots are tabulated in Table 1.

0.5% and 5% H_2 (Figure 6). Activation energies obtained from the slopes of these plots (slope $= -E_a/RT$) are characteristic of the chemical processes that limit the rates of sensor response and recovery (Table 2).

Let us consider first the response of the Pd nanowire to hydrogen. We measure activation energies of 4.1 ± 0.8 kcal mol^{-1} and 10.0 ± 0.7 kcal mol^{-1} for the response of the 94 × 183-nm nanowire to 0.5% and 5% H_2, respectively. These two activation energies can be expected to be different because in the case of the 5% H_2 exposure, the α-to-β phase transition occurs in parallel with H_2 dissociation and diffusion within the nanowire. An exposure to 0.5% H_2 does not induce this phase transition.[17] In Table 3 are tabulated literature values for the rates of the various chemical processes involved in H_2 absorption at Pd. Included in this table are values for adsorption and desorption at Pd surfaces that have been exposed to sulfur, which blocks adsorption sites for hydrogen at the Pd surface, simulating to some extent the contamination of the Pd nanowire surfaces in the present H_2 sensing experiments. The activation energy, E_a, for H diffusion in α-phase PdH_x, 5.3 kcal mol^{-1},[19] is close to the measured activation energy for 0.5% H_2 but H diffusion is much too rapid to limit the response or recovery of these nanowire-based H_2 sensors. This can be confirmed using Einstein's expression for the root mean square displacement, x, of a diffuser as a function of time, t: $x^2 = 2Dt$. Using the measured diffusion coefficient, D_H, for H in α-phase, nanocrystalline PdH_x (grain diameter ≈ 5 nm) at room temperature, $D_H = 5 \times 10^{-8}$ cm^2 s^{-1},[20] and the smallest dimension of the 94 × 183-nm nanowire evaluated in Figure 3, we calculate $t = 9 \times 10^{-4}$ s or about 1 ms; more than five orders of magnitude smaller than measured response and recovery times for this nanowire at room temperature (Figure 3b,c). This is the largest nanowire among those we fabricated for this study, and the diffusion coefficient for H in β-phase PdH_x is actually higher than that measured for bulk, microcrystalline PdH_x ($>5 \times 10^{-7}$ cm^2 s^{-1}[20]). We conclude that H diffusion is unlikely to limit the response or recovery rates for these devices at any H_2 concentration. The only other process involved in the response process at 0.5% H_2 is H_2 adsorption, which occurs with an E_a of 5.4 kcal mol^{-1} (clean Pd(110) [26]) and 6.8 kcal mol^{-1} (clean polycrystalline Pd,[27] Table 3). These E_a values were measured for rigorously clean Pd surfaces in a vacuum chamber whereas the surfaces of our Pd nanowires, which are exposed to laboratory air and aqueous plating solutions during the preparation of these sensors, are surely contaminated by strongly adsorbed molecules – water, hydrocarbons, and so on. To gauge the influence of strongly adsorbed molecules on the measured activation energies for the adsorption and desorption of H_2, Table 3 includes references to E_a values for sulfur-treated surfaces. The influence of sulfur on H_2 adsorption on Pd(110), for example, is to lower E_a from 5.4 to 3.4 kcal mol^{-1}.[21] Our measured response E_a of 4.1 ± 0.8 kcal mol^{-1} ($[H_2] = 0.5\%$) is somewhat lower than the 6.8 kcal mol^{-1} measured for H_2 adsorption on polycrystalline Pd, but this lower value is expected based upon the known effect of surface contamination of the Pd nanowire surface. For $[H_2] = 5\%$, we measure a higher E_a of 10.0 ± 0.7 kcal mol^{-1} that is consistent with the literature values for ΔH of the α → β phase transition, which ranges from 8.6 kcal mol^{-1}[22] to 9.8 kcal mol^{-1}.[23] While this analysis does not definitively identify the rate-limiting process in these two concentration regimes, we tentatively conclude that H_2 adsorption limits the response rate of these sensors for $[H_2] < \approx 1\%$ and higher H_2 concentrations imposes an additional, rate-limiting kinetic barrier associated with the α → β phase transition.

Table 2. Measured activation energies for the response and recovery of a Pd nanowire (94 × 183 nm) to H_2 at 0.5% and 5.0% in flowing N_2.

Process	H_2 concentration	E_a [kcal mol^{-1}]
Response	0.5%	4.1 ± 0.8
	5%	10.0 ± 0.7
Recovery	0.5%	10 ± 1
	5%	9.6 ± 0.5

Table 3. Literature values for the activation energy or enthalpy for four processes associated with H_2 adsorption and desorption on Pd.

Process	System	E_a [kcal mol^{-1}]	Ref.
H_2 adsorption	Pd(110) – clean	5.4	[26]
	Pd(110) – sulfur covered	3.4	[21]
	Pd foil – clean	6.8	[27]
H diffusion	Pd single crystal	5.3	[19]
H_2 desorption	Pd(100) – clean	20	[24]
	Pd(100) – sulfur covered	12	[24]
	Pd powder – clean	8.4	[25]
	Pd powder – sulfur covered	13	[25]
Process	System	$\Delta H_{\alpha\beta}$ [kcal mol^{-1}]	Ref.
α → β phase transition	bulk Pd	9.8	[23]
	bulk Pd	9.3	[28]
	Pd powder	8.6	[22]

The thermally activated sensor recovery rate produces a measured E_a of ≈10 kcal mol^{-1} at both 0.5% and 5% (Table 2). At 0.5% H_2, we expect H_2 desorption to limit the sensor recovery rate and our measured E_a is close to, but somewhat lower than, literature values for sulfur-contaminated Pd surfaces of 12–13 kcal mol^{-1}.[24,25] In the case of recovery from 5% H_2, we are unable to distinguish between the E_a of the H_2 desorption and the ΔH for the $\alpha \rightarrow \beta$ phase transition – either of these processes, or both, could impose the kinetic limit for sensor recovery.

3. Conclusions

Joule heating provides a means for accelerating the response and recovery rates of Pd nanowire-based hydrogen sensors while preserving the simplicity of the device. Three functions, 1) wire temperature measurement, 2) wire heating, and, 3) H_2 concentration measurement, are all carried out by a single Pd nanowire in this scheme. In this study, we observed accelerations of sensor response and recovery by factors of more than 50. Joule heating also reduced the sensitivity of the nanowire to H_2 by a factor of up to 38, but since a single Pd nanowire can readily detect 5 ppm H_2 at room temperature, the limit of detection of 100–500 ppm for the hot nanowire ($384\ K < T_{hot} < 428\ K$) is ample for safety sensors, according to recent DOE guidelines.[2] Importantly, Joule heating imparts the new ability for the smallest Pd nanowires to respond to >1% H_2 in less than 3 s while dissipating just 4 mW of power.

4. Experimental Section

Nanowire fabrication: Fracture-resistant Pd nanowires were fabricated using the 7-step LPNE procedure[12–14] as previously described.[8] The electrodeposition of Pd was carried out in a 50 mL, one-compartment, three-electrode cell using a platinum foil counter electrode and a saturated calomel reference electrode (SCE) in addition to the LPNE-fabricated working electrode. Pd nanowires were obtained by electroplating from a solution containing 0.1 M KCl, 0.2 mM $PdCl_2$, and 0.22 mM EDTA (pH = 3.8) at −0.8 V versus SCE. These plating solutions were prepared using Millipore MilliQ water ($\rho \geq 18\ M\Omega$). Nanowire deposition was controlled using a computer-controlled potentiostatic (Gamry Instruments G300 potentiostat/galvanostat).

Thermal calibration: A single Pd nanowire was heated in an infrared furnace (Model MILA-5000 Infrared Lamp Heating System, ULVAC-RIKO, Inc.) in nitrogen gas at 573 K for 30 min and then cooled to 294 K. The resistance of the Pd nanowire was monitored by a four-probe measurement during the temperature ramp up and down (data shown in Figure 2c) from 293 K to 550 K.

Hydrogen sensing: H_2 sensors were prepared by evaporating a four-probe gold electrode of 60-nm thickness onto single, linear nanowires of Pd using a contact shadow mask. The four-contact electrical resistivity was measured using a source meter (Keithley Instruments, model 2400) in conjunction with a digital multimeter (Keithley Instruments, model 2000), as shown schematically in Figure 1a. Sensor measurements were carried out by placing the sensor in a sealed flow cell with a total dead volume of 120 μL. H_2 gas (Airgas, minimum purity 99.998%) was mixed with N_2 (Airgas, minimum purity 99.998%) to a predetermined concentration using flow controllers (MKS Inc., model 1479A) and pulses of this gas mixture were switched (Parker Valve, cycle time = 25 ms) into a steam of pure N_2 (Airgas, minimum purity 99.998%) while maintaining a total flow rate of 1500 sccm. Instrument control and data acquisition were both coordinated by a computer equipped with Labview in conjunction with a National Instruments interface (model BNC 2110). All H_2 sensing measurements were carried out using dry gases at ambient laboratory temperature (≈294 K).

Finite element modeling: The temperature profile along the 100-μm-length nanowire was simulated with a finite element method (COMSOL Multiphysics 3.5a). The application module for Electro-Thermal Interaction was used for this 3D simulation.

Atomic force microscopy: Intermittent contact mode AFM images were acquired in air using an Asylum Research MFP-3D microscope and Olympus AC240TS tips.

Scanning electron microscopy: SEM measurements were carried out using a Philips model XL-30 FEG SEM operating at 15 keV and a working distance of 10 mm. All samples were sputter-coated with a thin (1–2 nm) gold film before imaging to prevent charging.

Acknowledgements

This work was supported by National Science Foundation Grant CHE-0956524 and the UCI School of Physical Sciences Center for Solar Energy. Valuable conversations with Profs. Mike Sailor (UCSD) and Gordon Miskelly (University of Auckland) are also acknowledged.

[1] V. Schroder, B. Emonts, H. Janssen, H. P. Schulze, *Chem. Eng. Technol.* **2004**, *27*, 847.
[2] Office of Energy Efficiency and Renewable Energy (EERE), The Department of Energy *Funding Opportunity Announcement: DE-PS36-09GO99004* The Department of Energy, Golden, CO, 2009.
[3] R. C. Hughes, W. K. Schubert, *J. Appl. Phys.* **1992**, *71*, 542.
[4] F. Favier, E. C. Walter, M. P. Zach, T. Benter, R. M. Penner, *Science* **2001**, *293*, 2227.
[5] E. C. Walter, F. Favier, R. M. Penner, *Anal. Chem.* **2002**, *74*, 1546.
[6] E. C. Walter, K. Ng, M. P. Zach, R. M. Penner, F. Favier, *Microelectron. Eng.* **2002**, *61*, 555.
[7] E. C. Walter, R. M. Penner, H. Liu, K. H. Ng, M. P. Zach, F. Favier, *Surface Interface Anal.* **2002**, *34*, 409.
[8] F. Yang, D. K. Taggart, R. M. Penner, *Nano Lett.* **2009**, *9*, 2177.
[9] Y. Im, C. Lee, R. P. Vasquez, M. A. Bangar, N. V. Myung, E. J. Menke, R. M. Penner, M. H. Yun, *Small* **2006**, *2*, 356.
[10] P. Offermans, H. D. Tong, C. J. M. van Rijn, P. Merken, S. H. Brongersma, M. Crego-Calama, *Appl. Phys. Lett.* **2009**, *94*, 22310.
[11] M. H. Yun, N. V. Myung, R. P. Vasquez, C. S. Lee, E. Menke, R. M. Penner, *Nano Lett.* **2004**, *4*, 419.

[12] E. J. Menke, M. A. Thompson, C. Xiang, L. C. Yang, R. M. Penner, *Nat. Mater.* **2006**, *5*, 914.
[13] C. X. Xiang, S. C. Kung, D. K. Taggart, F. Yang, M. A. Thompson, A. G. Guell, Y. A. Yang, R. M. Penner, *ACS Nano* **2008**, *2*, 1939.
[14] C. X. Xiang, Y. G. Yang, R. M. Penner, *Chem.Commun.* **2009**, 859.
[15] *CRC Handbook of Chemistry and Physics*, Chapman and Hall/CRCnetBASE, Boca Raton, FL **1999**.
[16] A. Sieverts, W. Danz, *Zeitschrift Fur Physikalische Chemie-Abteilung B-Chemie Der Elementarprozesse Aufbau Der Materie* **1937**, *38*, 46.
[17] F. A. Lewis, *The Pd Hydrogen system*, Academic Press, New York **1967**.
[18] F. A. Volkening, M. N. Naidoo, G. A. Candela, R. L. Holtz, V. Provenzano, *Nanostruct. Mater.* **1995**, *5*, 373.
[19] J. Volkl, G. Wollenwe, K. H. Klatt, G. Alefeld, *Zeitschrift Fur Naturforschung Part a-Astrophysik Physik Und Physikalische Chemie* **1971**, *A 26*, 922.
[20] T. Mutschele, R. Kirchheim, *Scripta Metallurgica* **1987**, *21*, 135.
[21] C. H. F. Peden, B. D. Kay, D. W. Goodman, *Surface Sci.* **1986**, *175*, 215.
[22] D. J. Barabino, C. Dybowski, *Sol. State Nucl. Magn. Res.* **1992**, *1*, 5.
[23] J. K. Jacobs, F. D. Manchester, *J. Phys. F.* **1971**, *4*, 129.
[24] M. L. Burke, R. J. Madix, *Surface Sci.* **1990**, *237*, 1.
[25] F. J. Castro, G. Meyer, G. Zampieri, *J. Alloys Compounds* **2002**, *330*, 612.
[26] B. D. Kay, C. H. F. Peden, D. W. Goodman, *Phys. Rev. B* **1986**, *34*, 817.
[27] W. Auer, H. J. Grabke, *Berichte Der Bunsen-Gesellschaft-Physical Chemistry Chemical Physics* **1974**, *78*, 58.
[28] H. Frieske, E. Wicke, *Berichte Der Bunsen-Gesellschaft-Physical Chemistry Chemical Physics* **1973**, *77*, 48.

Received: January 29, 2010
Revised: March 29, 2010
Published online: June 17, 2010

